

ESTIMATION OF HIV DYNAMIC PARAMETERS

HULIN WU^{*‡}, A. ADAM DING[†] and VICTOR DEGRUTTOLA[‡]

* Frontier Science & Technology Research Foundation, 1244 Boylston Street, Suite 303, Chestnut Hill, MA 02167-2104.

† Department of Mathematics, Northeastern University, Boston, MA 02115.

‡ Statistical and Data Analysis Center and Department of Biostatistics, Harvard School of Public Health, Boston, MA 02115.

SUMMARY

Investigation of HIV viral dynamics is important for understanding the HIV pathogenesis and for development of treatment strategies. Perelson et al.¹ demonstrated that simple viral dynamic models fit to data on viral load as measured by plasma HIV-RNA could produce estimates of rates of clearance of virus and of infected CD4⁺ T lymphocytes. In this paper we extend the work of Perelson et al. by proposing models with less restrictive assumptions about drug activity. Our models take into account the fact that both infectious and noninfectious virions are produced by infected T cells both before and after the treatment. We also show that direct measurement of infectious virus load provides sufficient information for estimation of antiretroviral drug efficacy parameter. For characterizing viral dynamics of populations and estimation of dynamic parameters, we propose a hierarchical nonlinear model. Compared to other methods such as the nonlinear least square method used by Perelson et al., we show that the proposed approach has the following advantages: 1) it is more appropriate for modeling within-patient and between-patient variation and to characterize the population dynamics; 2) it is flexible enough to deal with both rich and sparse individual data; 3) it has more power to detect model misspecification; 4) it allows incorporation of covariates for viral dynamic parameters; 5) it makes more efficient use of between-subject information to get better parameter estimates. We give two simulation examples to illustrate the proposed approach and its advantages. Finally, we discuss practical issues regarding the clinical trial design for viral dynamic studies.

1. INTRODUCTION

Results from mathematical models of HIV viral dynamics have considerably altered beliefs about rates of clearance of the virus itself and of the immune cells that the virus infects.¹⁻⁶

Investigation of viral dynamics is important for understanding the HIV pathogenesis and for the development of treatment strategies.

Simple models of viral dynamics were first used to estimate HIV-1 dynamic parameters using the viral load data from HIV-1 infected patients by Ho et al.² and Wei et al.³. Perelson *et al.*¹ extended the models to distinguish between the clearance rates of free virions and infected cells using the extensive viral load data during the first 2 days of treatment. An accurate mathematical treatment of the early phase (‘shoulder’) was given by Herz et al.⁷. Further extensions that considered imperfect drug and drug resistance were given by Nowak et al.⁸ and Bonhoeffer et al.⁹

Perelson *et al.*¹ proposed a simplified dynamic model to estimate HIV-1 dynamic parameters in vivo (the clearance rates of virus and productively infected T cells). Estimation of model parameters made use of sequential measurements of total virus load, as measured from plasma HIV-RNA, collected from five patients treated with an antiviral drug ritonavir—a potent protease inhibitor. Their model assumed that the HIV virions infect target T cells (T) and turn them into productively infected T cells (T^*). Each productively infected T cell is assumed to produce N virions in its life-time. The administration of ritonavir is assumed to cause all newly produced virions from the infected cells to be noninfectious during the study period. Therefore, only the infectious virions (V_I) produced before initiation of the drug effect can continue to infect the target T cells. As the infectious virions are eliminated continuously, the number of productively infected T cells declines. This results in a fall in the production of new noninfectious virions (V_{NI}); these virions are themselves eventually cleared. The dynamic model used in Perelson et al.¹ is as follows,

$$\frac{dT^*}{dt} = kTV_I - \delta T^*, \tag{1}$$

$$\frac{dV_I}{dt} = -cV_I, \tag{2}$$

$$\frac{dV_{NI}}{dt} = N\delta T^* - cV_{NI}. \tag{3}$$

Using this model, Perelson et al.¹ estimated the half-lives ($t_{1/2}$) of productively infected T cells and plasma virions as 1.6 days and 0.24 days respectively; these results are widely

used in the design of clinical trials and cited in the AIDS literature.

There are several problems in the model assumptions and in the estimation approach of Perelson et al.¹. First, the assumption that the concentration of noninfectious virions is 0 at time 0 [$V_{NI}(t = 0) = 0$], is incorrect. Although this assumption does not affect the closed-form solution of the amount of total virus and the parameter estimation based on it (Appendix I), it does affect the solutions for the infectious and non-infectious virus. The assumption does not appear correct, because the production of dysfunctional (non-infectious) virions from productively infected T cells is a natural phenomenon that exists even without any antiviral treatment. In fact, the number of infectious virions is believed to be much less than the noninfectious virions in the total virus pool.^{10–12} Therefore, it is inappropriate to ignore the existence of noninfectious virions before treatment. Secondly, no drug is likely to be perfect. Therefore, we cannot expect that all newly produced virions will be noninfectious after administration of ritonavir. Perelson et al.¹ suggested a modification to address this point in their references and notes. This modified model leads to a markedly different form of solution for the total concentration of plasma virions, $V = V_I + V_{NI}$, because the perfect drug case is a singular point of the system of differential equations for the imperfect drug case. As noted by Perelson et al.,¹ parameter estimates with perfect drug assumption are biased if the drug is actually imperfect. Thirdly, the nonlinear least square (NLS) regression analysis performed in Perelson *et al.*¹ does not use the data efficiently and cannot be applied to other settings, such as those where the measurements of virus load are infrequent for each individual patient.

In this paper we propose a modification to Perelson’s model by considering the fact that the infectious and noninfectious virions are produced by the infected T cells both before and after the treatment (i.e. drug is not perfect). We also introduce a more powerful hierarchical model approach to characterize the population HIV dynamics and to estimate the parameters. The advantages of our proposed approach are: (1) we model the population viral dynamics, within-patient and between-patient variations more appropriately; (2) the model has more flexibility to deal with both rich and sparse data for individuals; (3) covariates are easily incorporated in the viral dynamic parameters to explain between-patient variation; and (4) the model has more power to identify model misspecification

because we can use the cross-patient information. Advantage (2) is especially important in large clinical trials, because individual patient data are often sparse (collected infrequently) by necessity. This is also the case especially for some compartments such as lymph tissue, cerebrospinal fluid and CSF. The hierarchical model approach provides a tool to deal with this kind of sparse data by borrowing the cross-patient information.

In the next section, we propose our modified model. In Section 3, we introduce the hierarchical model approach. In Section 4 we investigate briefly the parameter identifiability and model diagnostics. We present two simulated numerical examples to illustrate our approach and to compare with the NLS method in Section 5. Finally, we offer conclusions and some discussion of practical issues and future research.

2. THE DYNAMIC MODELS

Let T , T^* , V_I and V_{NI} denote the concentration of target cells, productively infected cells, infectious virions and noninfectious virions respectively. Let $V = V_I + V_{NI}$ denotes the total concentration of virions. Following Perelson et al¹, we assume that the HIV infects the target cells with a constant rate k . We describe the interaction between the T cells and free HIV as:

$$\frac{dT^*}{dt} = kTV_I - \delta T^*, \tag{4}$$

$$\frac{dV}{dt} = N\delta T^* - cV, \tag{5}$$

where δ is the rate of loss of virus-producing cells, N is the number of new virions produced per infected cell during its lifetime, and c is the constant rate for virion clearance. If we consider a short time period, we may assume that the concentration of target T cells (T) is a constant.¹

To estimate parameters from equations (4) and (5), Perelson et al.¹ assumed that all the newly produced virions ($N\delta T^*$) are completely infectious before the treatment of a protease inhibitor and completely noninfectious after the treatment. For the reasons discussed in the previous section, we modify these equations by assuming that, before and after the treatment, respectively η_0 and η^* proportion of the newly produced virions are

infectious. Hence, the dynamics of the two categories of the virions are described by

$$\frac{dV_I}{dt} = (1 - \eta_0)N\delta T^* - cV_I, \quad (6)$$

$$\frac{dV_{NI}}{dt} = \eta_0 N\delta T^* - cV_{NI}, \quad (7)$$

before treatment. After treatment effect, we follow the suggestion of Perelson et al¹,

$$\frac{dV_I}{dt} = (1 - \eta^*)N\delta T^* - cV_I, \quad (8)$$

$$\frac{dV_{NI}}{dt} = \eta^* N\delta T^* - cV_{NI}. \quad (9)$$

As in Perelson et al.¹, if we assume that the protease inhibitor is perfect, i.e., $\eta^* = 1$, we can solve the above linear differential equations (with the quasi-steady state initial conditions) to obtain a closed form solution as follows (see Appendix I for details),

$$T^*(t) = \frac{c^2 V_0}{N\delta(c - \delta)} e^{-\delta t} - \frac{cV_0}{N(c - \delta)} e^{-ct}, \quad (10)$$

$$V_I(t) = V_0(1 - \eta_0)e^{-ct}, \quad (11)$$

$$V_{NI}(t) = V_0 \left\{ \frac{c^2}{(c - \delta)^2} e^{-\delta t} + \left[\frac{\eta_0(c - \delta)^2 - c^2}{(c - \delta)^2} - \frac{c\delta t}{c - \delta} \right] e^{-ct} \right\}. \quad (12)$$

Therefore the total virus is,

$$V(t) = V_I(t) + V_{NI}(t) = V_0 \left\{ \frac{c^2}{(c - \delta)^2} e^{-\delta t} + \left[1 - \frac{c^2}{(c - \delta)^2} - \frac{c\delta t}{c - \delta} \right] e^{-ct} \right\}. \quad (13)$$

Note that although we do not assume $V_{NI}(t = 0) = 0$, as did Perelson et al.¹, we obtain the same formula for total virus. However, this assumption does affect the results of $V_I(t)$ and $V_{NI}(t)$ in (11) and (12).

In the more plausible case that $\eta^* \neq 1$ (imperfect drug), we define $\eta = (\eta^* - \eta_0)/(1 - \eta_0)$, as the efficacy of the protease inhibitor drug relative to a perfect drug. Notice that the $(\eta^* - \eta_0)$ is a measurement of the current drug effect, and simply equals $(1 - \eta_0)$ for perfect drug, $\eta^* = 1$. Similarly we can solve the system of linear differential equations (4), (8) and (9), and use the steady-state conditions derived from (4), (6) and (7) (see Appendix II for details) to obtain

$$T^* = \frac{T_0^*}{2} [a_1 \exp(-d_1 t) + a_2 \exp(-d_2 t)],$$

$$\begin{aligned}
V_I(t) &= \frac{V_{I0}}{2}[a_3 \exp(-d_1 t) + a_4 \exp(-d_2 t)], \\
V_{NI}(t) &= \frac{\eta V_{I0} + V_{NI0}}{2(1-\eta)}[a_3 \exp(-d_1 t) + a_4 \exp(-d_2 t)] - \frac{\eta V_0}{(1-\eta)} \exp(-ct),
\end{aligned} \tag{14}$$

where

$$\begin{aligned}
a_1 &= 1 + \frac{c + \delta}{\sqrt{(c + \delta)^2 - 4c\delta\eta}}, & a_2 &= 1 - \frac{c + \delta}{\sqrt{(c + \delta)^2 - 4c\delta\eta}}, \\
a_3 &= 1 + \frac{\delta + c - 2c\eta}{\sqrt{(c + \delta)^2 - 4c\delta\eta}}, & a_4 &= 1 - \frac{\delta + c - 2c\eta}{\sqrt{(c + \delta)^2 - 4c\delta\eta}}, \\
d_1 &= \frac{(c + \delta) - \sqrt{(c + \delta)^2 - 4c\delta\eta}}{2}, & d_2 &= \frac{(c + \delta) + \sqrt{(c + \delta)^2 - 4c\delta\eta}}{2},
\end{aligned}$$

and the total concentration of virions,

$$V(t) = \frac{V_0}{2(1-\eta)}[a_3 \exp(-d_1 t) + a_4 \exp(-d_2 t)] - \frac{\eta V_0}{(1-\eta)} \exp(-ct). \tag{15}$$

In Section 4, we show that we cannot identify the three parameters c , δ and η simultaneously using only the measurements of total virus, $V(t)$, $t = 1, 2, \dots, n$. However, if we have sequential measurements of infectious virions, $V_I(t)$, we may easily identify these parameters using the formula for V_I in (14) (see next two sections). In the next section, we propose using hierarchical nonlinear models (HNM) to estimate the parameters.

3. HIERARCHICAL NONLINEAR MODELS AND PARAMETER ESTIMATIONS

For estimation, Perelson et al.¹ simply used the NLS regression to fit their data for each individual patient separately and they obtained parameter estimates for each individual. The NLS approach does not account for the within- and between-patient variation appropriately and does not use the cross-patient information efficiently. The simple averages of individual parameter estimates are not good estimates for population parameters, though some two-stage methods may be used to improve the population parameter estimates.^{13,14} Here we propose using hierarchical nonlinear models (HNMs) to model population HIV dynamics, the within-patient and between-patient variations. Therefore we can take advantage of the HNM approach: flexibility to deal with rich and sparse individual data,

ability to incorporate the covariates, and efficient utilization of cross-patient information. Since its first introduction to pharmacokinetics/pharmacodynamics by Sheiner, Rosenberg and Melmon¹⁵ in 1972, the HNM has been widely used in biological studies.^{13,16} A general HNM is described as follows. For the i th patient,

Stage 1, within-patient variation

$$\mathbf{y}_i = \mathbf{f}(\mathbf{x}_i, \boldsymbol{\beta}_i) + \mathbf{e}_i, \quad \mathbf{e}_i | \boldsymbol{\beta}_i \sim (\mathbf{0}, \mathbf{R}_i(\boldsymbol{\beta}_i, \boldsymbol{\xi})),$$

Stage 2, between-patient variation

$$\boldsymbol{\beta}_i = \mathbf{d}(\mathbf{a}_i, \boldsymbol{\beta}, \mathbf{b}_i), \quad \mathbf{b}_i \sim (\mathbf{0}, \mathbf{D}),$$

where \mathbf{y}_i and \mathbf{e}_i are $(n_i \times 1)$ vectors of responses (measurements) and within-patient random errors for individual i with n_i measurements. (We use bold letters to denote the vectors in this paper.) The vector function $\mathbf{f}(\mathbf{x}_i, \boldsymbol{\beta}_i) = [f(\mathbf{x}_{i1}, \boldsymbol{\beta}_i), \dots, f(\mathbf{x}_{in_i}, \boldsymbol{\beta}_i)]'$ is the mean function for i th individual with the $(p \times 1)$ individual-specific regression parameter vector $\boldsymbol{\beta}_i$ and independent variables \mathbf{x}_i (usually time t). Here $\mathbf{d}(\mathbf{a}_i, \boldsymbol{\beta}, \mathbf{b}_i)$ is a p -dimensional function of between-patient covariate vector \mathbf{a}_i , population parameter vector $\boldsymbol{\beta}$ and between-patient random error \mathbf{b}_i . This function may be linear or nonlinear (see Davidian and Giltinan¹³ for details).

In our case \mathbf{y}_i is the measurement of viral load or the number of infected T cells for the i th patient, \mathbf{e}_i is the within-patient random measurement error. The mean function $\mathbf{f}(\mathbf{x}_i, \boldsymbol{\beta}_i)$ is $V_I(t)$, $V_{NI}(t)$, $V(t)$, or T^* as in (14) or (15) depending on what is measured. The independent variable \mathbf{x}_i is time t . The parameters for each individual patient are $\boldsymbol{\beta}_i = [c_i, \delta_i, \eta_i]'$ in our model (14) or (15), and we may simply assume that they are the population parameters (fixed effects) with additive between-patient random error, say, $\boldsymbol{\beta}_i = \boldsymbol{\beta} + \mathbf{b}_i$, where $\boldsymbol{\beta} = [c, \delta, \eta]'$ is the population parameters. Notice that we shall scale $V(t)$ or $V_I(t)$ by dividing V_0 or V_{I0} in our simulation examples; and after scaling in this way, we do not need to estimate the initial value, V_0 or V_{I0} , in the formula (14) or (15), i.e., we fit the ratio of virus load to its initial values (we can also treat V_0 or V_{I0} as unknown parameters as in Perelson et al.¹).

More complicated models (such as nonlinear model with multiplicative random errors) can be used for function $\mathbf{d}(\mathbf{a}_i, \boldsymbol{\beta}, \mathbf{b}_i)$. Covariates \mathbf{a}_i such as baseline values, age and weight

of patients, complement activity, etc., can be incorporated. For example, the parameter of clearance rate c and/or δ , may depend on the baseline virus load, age of the patient and other individualized variables. Then the HNM can be used to study the effect of these covariables to these viral dynamic parameters. For example, we can assume that $\boldsymbol{\beta}_i = \mathbf{A}_i\boldsymbol{\beta} + \mathbf{B}_i\mathbf{b}_i$ (or even other nonlinear functions), where \mathbf{A}_i and \mathbf{B}_i are design matrices (or covariates) for the fixed and random effects respectively, which contain the covariate information of the i th patient such as baseline values and age of patients.

One usually assumes that the within-patient random errors (measurement errors) \mathbf{e}_i have mean $\mathbf{0}$ and variance-covariance structure $\mathbf{R}_i(\boldsymbol{\beta}_i, \boldsymbol{\xi})$, and are independent between patients. A simple choice is $\mathbf{R}_i(\boldsymbol{\beta}_i, \boldsymbol{\xi}) = \sigma^2 \text{diag}[f^2(\mathbf{x}_{i1}, \boldsymbol{\beta}_i), \dots, f^2(\mathbf{x}_{in_i}, \boldsymbol{\beta}_i)]$. We assume that the between-patient random errors \mathbf{b}_i have mean 0 and are i.i.d. with a common covariance matrix \mathbf{D} . For these two random errors, if we assume a distribution (say, normal or lognormal), we can use the maximum likelihood inferences. However, if not, we can use the generalized least square approach for parameter inferences.

Two classes of inferential procedures have been proposed for the HNMs. One is based on individual-specific regression parameter estimates when there are sufficient measurements taken on individuals to allow estimation of individual parameters. In this case, one can estimate the population parameters using the standard two-stage method (STS), the global two-stage method (GTS), the iterated two-stage method (ITS) or Bayesian method. A brief review of these methods appear in the book by Davidian and Giltinan¹³ (Chapter 5) and Steimer et al.¹⁷ Also see Steimer et al.¹⁴ for some comparisons of these methods.

Another class of inferential procedures is based on linearization (Davidian and Giltinan¹³, Chapter 6). We use this approach in our numerical examples because it is more suitable for settings where individual data are sparse. The nonparametric, semiparametric and Bayesian approach have also been developed for the HNMs. We refer readers for the details of these inferential methods to Davidian and Giltinan¹³. Several computer packages or functions such as SAS, Splus, NONMEM, P-Pharm are developed for the inferences of HNMs. In this paper, we use the Splus function, NLME, developed by Pinheiro and Bates.¹⁸

When we obtain the estimates for parameters (c, δ, η) , we may also estimate other parameters in the model using the steady-state condition at the initial time points. From the steady-state equations (20)-(22) in Appendix I, we can obtain that

$$k = \frac{\delta T_0^*}{TV_{I_0}}, \quad N = \frac{cV_0}{\delta T_0^*}. \quad (16)$$

Thus if we can obtain the initial values of infectious virus, total virus, productively infected T cells, and uninfected T cells by assays, we can also estimate the infection rate k and the number of virions produced by a productively infected T cell in its life time, N .

4. PARAMETER IDENTIFIABILITY AND MODEL DIAGNOSTICS

Before we illustrate the application of HNMs to estimate the HIV dynamic parameters using numerical examples, we briefly investigate the parameter identifiability and model diagnostics in this section. We show that if only total virus is measured, we cannot identify all the parameters in imperfect drug case. If infectious virus can be measured (as is now possible, Scott Hammer, personal communication), these parameters are identifiable. In addition to demonstrating the conditions for parameter identifiability, we show from a numerical example that the HNM approach has more power than other approaches to detect model misspecification.

4.1. Parameter identifiability

The dynamic model in previous sections provides a way to estimate the clearance rates (c and δ) of free virus and productively infected T cells, and drug efficacy η from virus load data. By repeated measurement of the total virus load before and after initiation of treatment, we can estimate the parameters based on formulas (13), (14) or (15) depending on the assumptions and measurements. Perelson *et al.*¹ applied the NLS method to fit the model (13) for the viral load data *in vivo* and to estimate the clearance rates c and δ under the assumption of a perfect drug ($\eta = 1$).

If we want to estimate η , however, there is a problem with parameter identifiability. As mentioned in Section 2, the parameters are not completely identifiable if $\eta \neq 1$ and

we have only measurement of total virus. Although the parameters are theoretically identifiable from the total viral load using formula (15), they are not estimable in practice because of measurement error. The reason is that many different sets of parameters in formula (15) may produce mathematically different $V(t)$ curves, but the differences are too small to be identified based on the observed data with random errors.

In practice, the viral clearance rate c usually is much larger than the clearance rate of the infected T cells, δ . (In Perelson *et al.*¹, the two estimates differ by a factor between 5 and 10.) Since the protease inhibitors are usually very potent, one often assume η is close to 1. In such situations, the total viral load (15) is a sum of three exponential terms. However, the exponential rates for the last two terms are almost the same and their coefficients are of opposite signs with approximately same magnitude. Thus the sum of the last two exponential terms is small compared to the first. For example, if we take $\beta_1 = (\eta_1, c_1, \delta_1) = (0.8, 3.0, 0.5)$, the sum (scaled by dividing V_0) of the last two terms in (15) is,

$$\begin{aligned} & \frac{1}{2(1-\eta)} \left[\left(1 - \frac{\delta+c-2c\eta}{\sqrt{(c+\delta)^2-4c\delta\eta}} \right) \exp\left(\frac{-(c+\delta)-\sqrt{(c+\delta)^2-4c\delta\eta}}{2}t\right) - 2\eta \exp(-ct) \right] \\ &= 3.691e^{-3.115t} - 4e^{-3t}, \end{aligned}$$

which goes to a very small value as time t increases. But the first exponential term in (15) is $1.309e^{-0.385t}$ in this case, which dominates the total viral load process. Thus three parameters are nearly redundant and cannot be identified simultaneously.

In the following, we show that two different sets of parameters may lead to the similar total virus curves. In Figure 1, we plot the two curves of $V(t)$ from (15) using the two different parameter sets, $(\eta_1, c_1, \delta_1) = (0.8, 3.0, 0.5)$ and $(\eta_2, c_2, \delta_2) = (0.5, 2.812, 0.916)$. These two curves cannot be identified. In fact, they are two different curves, but the difference between them is too small. We sampled 16 time points from the two curves following the time schedule of Perelson *et al.*¹, the sum of squares of the differences between the two curves on these 16 time points is only 0.005. However, the measurement error of viral load (the coefficient of variation, CV, is 10% to 20%) is at least 1000-fold bigger than this value. Thus these two different parameter sets are numerically unidentifiable using the measurements of total viral load.

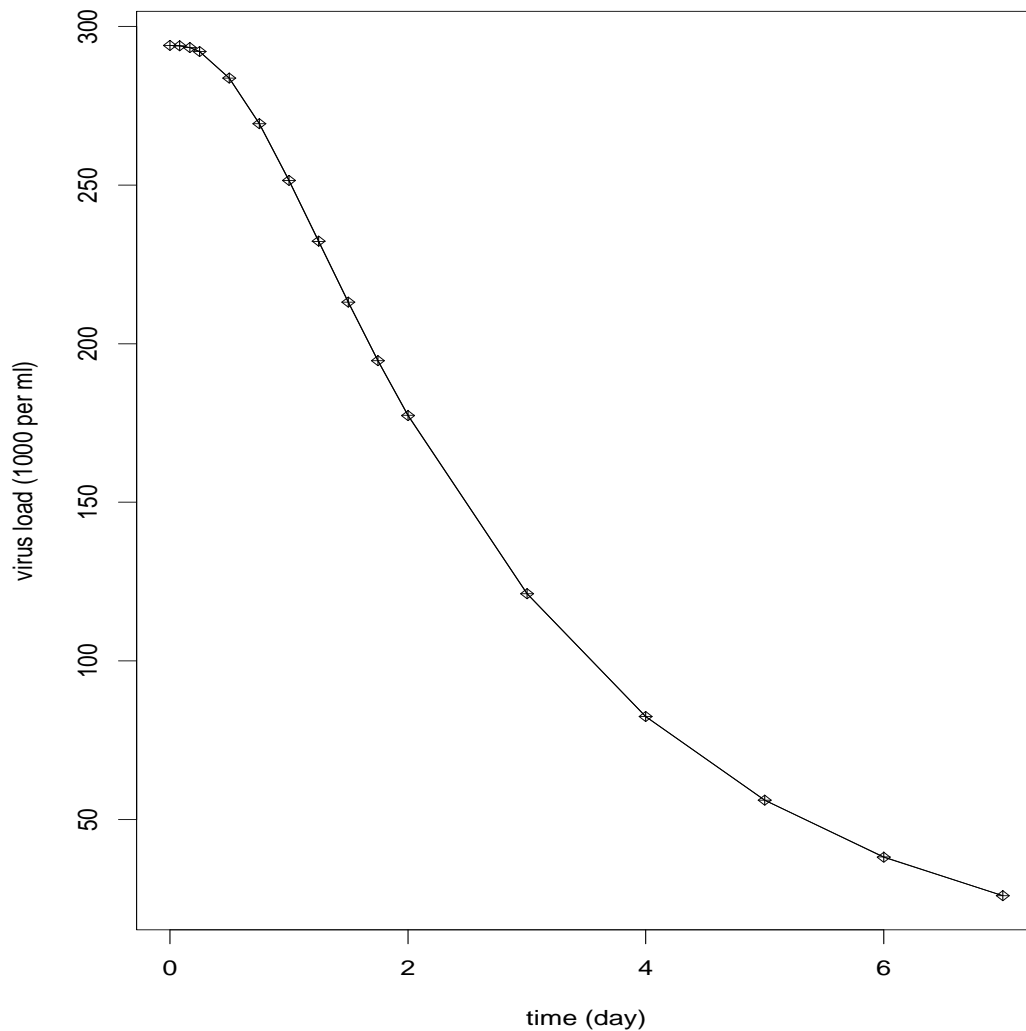


Figure 1: The solid line is the curve of (15) with parameters $\beta_1 = (0.8, 3.0, 0.5)$, where \diamond are the points of the curve at the same times as that of measurements for each individual patient in Perelson et al.¹. The crosses “+” are the virus load at the same time points, but produced from the curve with another parameter set, $\beta_2 = (0.5, 2.812, 0.916)$.

The above example shows that the information contained in the total viral load measurements is not enough for identifying all the three parameters (η, c, δ) . To identify the drug efficacy as well as the clearance rates of virus and infected T cells, more information such as the concentration of infectious virions (V_I) is needed. The measurements, $V_I(t)$, provide further information on the HIV dynamics and enable us to estimate all the parameters based on the solution (14). For example, the solution for $V_I(t)$ is a sum of two exponential terms with very different decay rates; this solves the identifiability problem. For $\beta_1 = (0.8, 3.0, 0.5)$, $V_I(t) = V_{I0}(0.26186e^{-0.3853t} + 0.73814e^{-3.1147t})$. The two exponential rates differ by a factor of 10 and thus are very easy to distinguish. From the numerical examples in the next section, we can see that we can also estimate drug efficacy based on such extra information.

4.2. Model diagnostics

As mentioned in the introduction, the HNM approach is more powerful for model diagnostics since we can use the cross-patient information. When people fit each individual's viral dynamic data using the NLS method, only individual data are applicable for each individual model diagnostics. This may not be powerful enough to identify the model misspecification in some cases, especially for the case of sparse data on each individual. Thus this may result in misleading diagnostic conclusions. In this subsection, we show this point using a simulation example.

This numerical example is similar to Example 2 in next section except that we add 4 more time-point measurements (on Day 10, 14, 21, and 28) and we use the perfect drug model. In this case we obtain richer individual data and this benefits the NLS approach. We expect that the comparison between the NLS and HNM approaches is fair.

First we simulate the observed data, total virus load, from Perelson's perfect drug model¹ or equation (13). Secondly we simulate another data set from another model specified by the following differential equations,

$$\frac{dT^*}{dt} = kTV_I - \delta T^*, \quad (17)$$

$$\frac{dV_I}{dt} = -cV_I \log(V_I^{0.1}), \quad (18)$$

$$\frac{dV_{NI}}{dt} = N\delta T^* - cV_{NI} \log(V_{NI}^{0.1}). \quad (19)$$

In this model, the virus clearance does not follow an exponential as in Perelson et al.¹. Instead we specify it as a double exponential which seems to fit some clinical data. We simulate the data from this model using numerical integration (Splus initial value problem function, “ivp.ab”), and we add the random measurement error as that in Example 2 in next section.

We fit these two data sets to the same model (13). Our purpose is to see whether the model diagnostic tools such as residual plots can identify that the second data set is from a wrong model. Following Perelson et al.¹, we simulated data for five subjects (see examples in next section for detailed simulation procedure). First we separately fit the total virus load data for these 5 subjects using the NLS approach (for both right model and wrong model data). And then we fit the five subjects’ data using the population HNM approach.

For the NLS approach, two out of 5 subjects’ data from both right and wrong models are successfully fitted. We show the residual versus fitted value plots in Figure 2 (the right model in Figure 2a and 2b and the wrong model in Figure 2c and 2d). There are no clearly abnormal patterns seen in Figure 2(c) and 2(d). From these plots, it is impossible to identify the wrong model.

For the HNM approach, however, we fit both data sets successfully, although the estimate of virus clearance rate is very large for the wrong model. We plot the residuals versus fitted values in Figure 3. From the right model data, the residual plot in Figure 3(a) shows no pattern, and for the wrong model data, the plot in Figure 3(b) shows a very clear abnormal pattern.

This example shows that the HNM approach has more power to detect model misspecification compared to the NLS approach when we use the residual versus fitted value plots. More theoretical and comprehensive studies on model diagnostics are needed.

5. NUMERICAL EXAMPLES

To illustrate the approaches proposed in this paper and to show its advantages com-

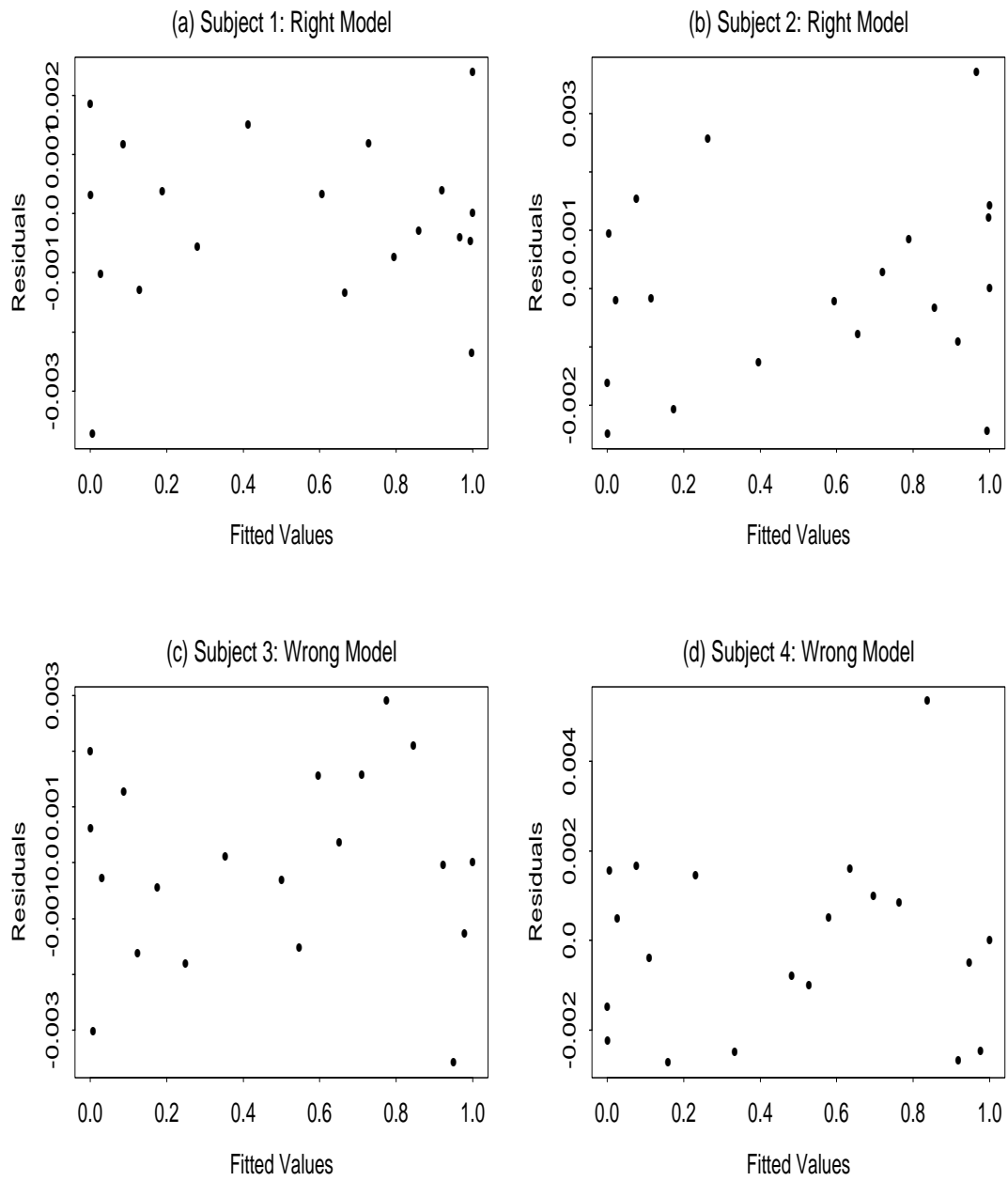


Figure 2: The NLS residual plots for right model (a and b) and wrong model (c and d).

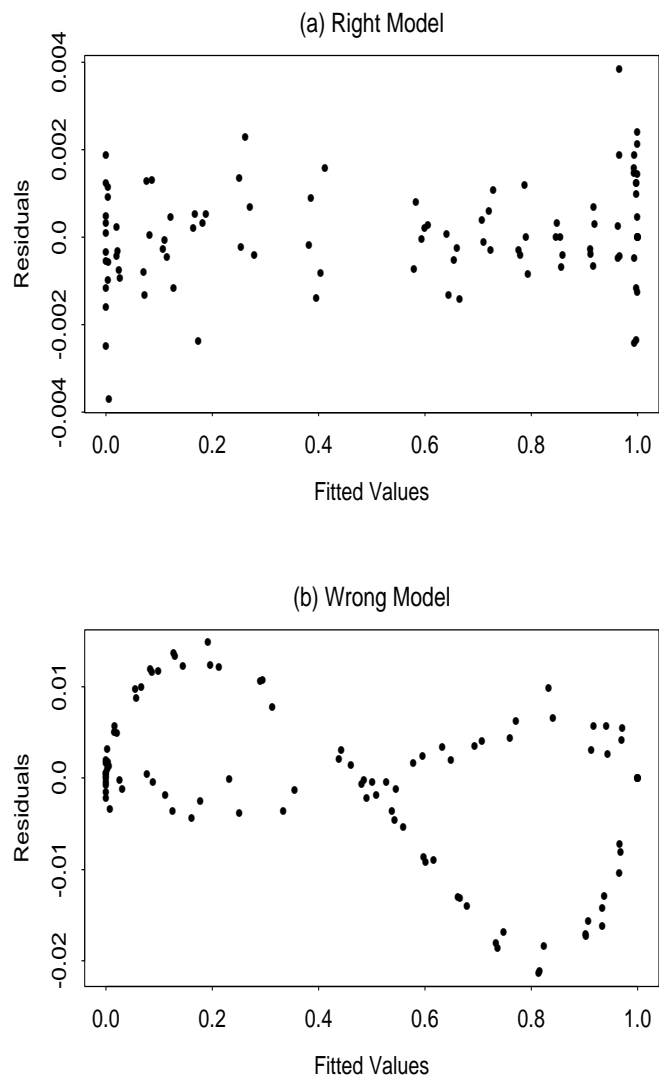


Figure 3: The HNM residual plots for right model (a) and wrong model (b).

pared with other methods, we present two simulated numerical examples. In the first example, when $\eta = 1$ (perfect drug case), we show that the clearance rates of infected T cells and free virus can also be well estimated based on sparse measurements of total virus load $V(t)$ using the HNM approach. In this example we also investigate the covariate effects on the viral dynamic parameters. We show that we can identify the covariates successfully using the AIC, BIC or other model selection criteria. In Example 2, we illustrate that we can identify the drug efficacy parameter, η , together with other two viral dynamic parameters provided we can measure infectious virus concentration. We also show that the consequence of an incorrect assumption of perfect drug when η is only .8, is that the bias and mean-squared error (MSE) are unacceptably large. Using this experiment, we also compare the HNM and NLS estimation methods for the imperfect drug model. The bias of the two approaches is similar, but the MSE of HNM estimates is consistently smaller than that of the NLS estimates for both the population and individual parameters.

Example 1. In this example we simulate a clinical trial with 40 HIV infected patients in a short time period (10 days) of protease inhibitor monotherapy treatment. For each patient we assume that four measurements of virus load are taken in the treatment period (Entry day 0, Day 2, Day 7, and Day 10). The design of this simulation experiment is based on an actual AIDS clinical trial (ACTG 315), from which we can develop the viral dynamic models. We assume, as in Perelson et al.¹, that the protease inhibitor drug is perfect and that other assumptions in Perelson et al.¹ are also satisfied. Thus, we can use the perfect drug model (13) to analyze the data.

We generate the true parameters using the following between-patient variation model

$$c_i = c + \beta_1 V_{i0} + b_{1i}, \quad \delta_i = \delta + \beta_2 V_{i0} + b_{2i},$$

where c_i and δ_i are the clearance rate of the free virus and productively infected T cells respectively for i th patient ($i = 1, 2, \dots, 40$). We assume that these two parameters are the linear functions of population parameters ($c = 3.0$ and $\delta = 0.4$) and the baseline virus load V_{i0} (the V_{i0} is scaled by dividing by 120000 in our simulation, and $\beta_1 = 2.0, \beta_2 = 0.2$). We assume that the random effects, b_{1i} and b_{2i} are normal distributions with mean 0 and

standard deviations of 0.1 and 0.03 respectively. We generate the baseline virus load, V_{i0} , using a uniform distribution with range of (5000,250000) for the 40 patients. Based on the results in Ho et al.² and Wei et al.³, the viral clearance (decay) rate and the baseline virus load are not correlated, and our simulation example shows that, if they are correlated, we are able to identify it using our approach.

To further the study of covariate effect on the clearance rates, we generate an extra covariate, the “age of patients” which is uncorrelated with two clearance rates in the model. We generate this covariate using an uniform distribution with a range of (25,60). We also fit a model with this additional covariate, to determine whether model selection techniques such as AIC or BIC appropriately select models without this covariate.

In this example we assume that only total virus load is measured and is the only information for parameter estimation. The observations (the total virus load) are generated using the formula (13) with the above generated parameters and an additive within-patient measurement error,

$$\mathbf{y}_i = V(c_i, \delta_i, t) + \mathbf{e}_i,$$

where $V(c_i, \delta_i, t)$ is the total virus load function (13) and we assume that the within-patient random error \mathbf{e}_i is normally distributed with zero mean and constant standard deviation 100. Actually, one may use a more complicated random measurement error model. For example, we may use the multiplicative error or model the variance of the error as a function of the mean.¹³ Here we keep it simple for illustrative purpose.

We use the generated observations to estimate the viral dynamic parameters by applying the approach introduced in Section 3. For simplicity, we scale the observations $V(t)$ by dividing V_0 . Thus, the value, V_0 , is not estimated. We fit three different models. The first is a model without considering any covariate for the between-patient variation. The second is the true model, i.e., we consider the covariate V_{i0} . In the third model we consider an additional unnecessary covariate “AGE” of the patients as well as the necessary covariate V_{i0} . We replicated the experiment 100 times with results summarized in Table 1.

In Table 1, we report only population parameter estimates, but we can also obtain the parameter estimates for each individual patient using empirical Bayes methods. We ob-

Table 1: The results for three hierarchical nonlinear models with 100 replications. S.E. denotes the square root of mean-squared error (MSE), The % is based on the true value.

Model 1	$c_i = c + b_{1i}$		$\delta_i = \delta + b_{2i}$			
True	$c = 5.125$		$\delta = 0.6125$			
Mean Estimate	5.048		0.6135			
Bias	-0.077		0.00097			
Bias (%)	-1.5%		0.2%			
S.E.	0.244		0.0201			
S.E. (%)	4.8%		3.3%			
95% CI Coverage	85%		90%			
AIC Selection	0		BIC	Selection	0	
Model 2	$\delta_i = \delta + \beta_2 V_{i0} + b_{2i}$		$\delta_i = \delta + \beta_2 V_{i0} + b_{2i}$			
True	$c = 3$	$\beta_1 = 2$	$\delta = 0.4$	$\beta_2 = 0.2$		
Mean Estimate	3.00036	2.0135	0.40034	0.1989		
Bias	0.00036	0.0135	0.00034	-0.0011		
Bias (%)	0.012%	0.7%	0.1%	-0.5%		
S.E.	0.1648	0.2372	0.0117	0.0100		
S.E. (%)	5.5%	11.9%	2.9%	5.0%		
95% CI Coverage	75%	90%	90%	92%		
AIC Selection	84		BIC	Selection	99	
Model 3	$c_i = c + \beta_1 V_{i0} + \beta_3 \text{AGE} + b_{1i}$			$\delta_i = \delta + \beta_2 V_{i0} + \beta_4 \text{AGE} + b_{2i}$		
True	$c = 3$	$\beta_1 = 2$	$\beta_3 = 0$	$\delta = 0.4$	$\beta_2 = 0.2$	$\beta_4 = 0$
Mean Estimate	3.020	2.0179	-0.0186	0.4003	0.1990	-0.0003
Bias	0.020	0.0179	-0.0186	0.0003	-0.0010	-0.0003
Bias (%)	0.7%	0.9%		0.1%	0.5%	
S.E.	0.3495	0.2502	0.3662	0.0242	0.0096	0.0254
S.E. (%)	11.7%	12.5%		6.1%	4.8%	
95% CI Coverage	90%	88%	89%	96%	93%	95%
AIC Selection	16			BIC	Selection	1

tained the maximum likelihood estimates for parameters using the Splus function NLME developed by Pinheiro and Bates¹⁸.

The simulation results show that the bias of parameter estimate is very small (less than 1.5%) for all three models. The standard estimate error (S.E.), defined as the square-root of MSE, is reasonable (less than 12.5% of the true value). The estimate of infected T cell clearance rate is consistently better than that of free virus clearance rate in terms of the S.E.. Note that the NLME Splus function also outputs the standard error of the estimates. This standard error estimate is based on the Fisher information, which is the lower bound of the standard error under the asymptotic theory. Using this standard error estimate and under the asymptotic normality assumption, we obtain the 95% confidence interval coverages in the 100 replications. The coverage should be smaller than 95% in general unless the standard error estimate is exaggerated. For most parameters, the coverage is reasonable except for parameter c in Model 2 where the coverage is only 75%. We suspect that this low coverage may also be caused by the truncation in our simulation (we dropped the case if the simulated data had too many outliers where we could not fit any one of the three models successfully). We note that one may obtain a more accurate estimate of the standard deviation using the bootstrap method, but it costs much more in computation.

In Table 1, we also present the number of times that we selected the model as best by AIC and BIC criteria. Based on our results, the BIC criterion is better behaved (99% of the correct model selection) than that of the AIC (84% of the correct model selection). But both criteria tend to include more covariates when we select the wrong model. Model 1 is never selected by either criterion. From this example, we can see that we can also use the hierarchical model approach to identify the important factors that may explain some of the between-patient variations of dynamic parameters.

Example 2. To illustrate the identification of drug efficacy for imperfect drug using the information of infectious virus measurements and to evaluate the consequence of misapplication of perfect drug assumption, in this example we follow Perelson et al.¹ to consider 5 patients in the experiment and 16 time-point measurements for each patient

as scheduled as that in Perelson et al.¹ However, here we assume that the drug efficacy, η is only .8 rather than 1.0. As indicated in the last section, the parameters cannot be completely identified for the imperfect drug case using only the measurement of total virus load. In this example we assume that we can quantify the infectious virus and that we have sequential measurements of infectious virus load. We illustrate that we can identify all the HIV dynamic parameters (including drug efficacy) in the model.

The true dynamic parameters, c_i and δ_i , are generated by $c_i = c + b_{1i}$ and $\delta_i = \delta + b_{2i}$, where $c = 3.0$ and $\delta = 0.5$ are population parameters, the b_{1i} and b_{2i} are random effects following normal distributions with mean 0 and standard deviations of 0.64 and 0.13 respectively as estimated in Perelson et al.¹ Because there are no covariates in this example, the between-patient variation is completely due to unexplained random effects; relative drug efficacy is a fixed effect, $\eta = 0.8$ for all the patients. We generated the baseline total virus loads (the viral loads at time 0) using the uniform distribution as in Example 1, and assume that the baseline infectious virus load is 0.1% of total virus at time $t = 0$, or $V_{I0} = 0.001V_0$. We simulate the measurements of infectious virus using the formula $V_I(t)$ in (14) with multiplicative normal random error (CV=15%). Similarly as in other examples, we fitted the observed ratio, $V_I(t)/V_{I0}$. The natural log scale is used in this example, due to multiplicative measurement error. The experiment is replicated 100 times. Table 2 summarizes the population and individual parameter estimates (the individual estimates are empirical Bayes estimates).

From the results in Table 2, when we fit the right model of infectious virus load, the bias of estimates is very small (for the population parameter estimates, the bias ranged from 0.6% to 3.8%; for the individual parameter estimates, the bias ranged from 0.6% to 9.2%). The S.E. (squared-root of MSE) of the estimates are reasonable (ranges from 2.1% to 12.6% for population estimates and from 5.9% to 30% for individual estimates) considering that CV of measurement error is 15%. Generally speaking, the population parameter estimates are better than the individual parameter estimates. This is expected because we have more information to estimate the population parameters. As with the previous example, the estimates of clearance rate of infected T cells are consistently better than those of free virus in terms of bias and MSE for both population and individual

Table 2: The results for imperfect drug data and misapplication of perfect drug model: 100 replications. (S.E. denotes the square root of MSE. The % is based on the true value).

Model 1:	Fit $V_I(t)$ model with considering the fact of imperfect drug				
	True Value	Mean Est.	Bias (%)	S.E. (%)	95% CI Cover
Population	$c = 2.837$	2.730	-0.107 (-3.8%)	0.359 (12.6%)	96%
	$\delta = 0.522$	0.511	-0.011 (-2.1%)	0.032 (6.1%)	100%
	$\eta = 0.8$	0.804	0.004 (0.6%)	0.017 (2.1%)	86%
Patient 1	$c = 3.621$	3.432	-0.189 (-5.2%)	0.840 (23.2%)	
	$\delta = 0.564$	0.548	-0.016 (-3.0%)	0.040 (7.1%)	
Patient 2	$c = 3.152$	2.905	0.247 (7.8%)	0.854 (27.1%)	
	$\delta = 0.708$	0.704	-0.004 (-0.6%)	0.042 (5.9%)	
Patient 3	$c = 1.241$	1.328	0.087 (7.0%)	0.273 (22.0%)	
	$\delta = 0.402$	0.387	-0.015 (-3.8%)	0.045 (11.3%)	
Patient 4	$c = 3.146$	2.858	-0.288 (-9.2%)	0.943 (30.0%)	
	$\delta = 0.251$	0.247	-0.004 (-1.6%)	0.035 (13.8%)	
Patient 5	$c = 3.026$	3.129	-0.103 (-3.4%)	0.688 (22.7%)	
	$\delta = 0.685$	0.672	-0.013 (-1.9%)	0.042 (6.2%)	
Model 2:	Mistakenly fit perfect drug model, $V(t)$				
Population	$c = 2.837$	2.926	0.089 (3.1%)	1.113 (39.9%)	88%
	$\delta = 0.522$	0.432	-0.090 (-17.2%)	0.121 (23.2%)	53%
Patient 1	$c = 3.621$	3.542	-0.078 (-2.2%)	2.274 (62.8%)	
	$\delta = 0.564$	0.450	-0.114 (-20.2%)	0.121 (21.5%)	
Patient 2	$c = 3.152$	2.985	-0.167 (-5.3%)	1.444 (45.8%)	
	$\delta = 0.708$	0.535	-0.173 (-24.4%)	0.182 (25.7%)	
Patient 3	$c = 1.241$	2.211	0.970 (78.2%)	2.385 (192.2%)	
	$\delta = 0.402$	0.363	-0.039 (-9.7%)	0.172 (42.8%)	
Patient 4	$c = 3.146$	2.724	-0.422 (-13.4%)	2.283 (72.6%)	
	$\delta = 0.251$	0.288	0.037 (14.9%)	0.156 (62.3%)	
Patient 5	$c = 3.026$	3.167	0.141 (4.7%)	1.283 (42.4%)	
	$\delta = 0.685$	0.521	-0.164 (-23.9%)	0.166 (24.3%)	

parameters. The reason for this is not completely clear, but it may be due to the nonlinear structure of the model. Also we can see that the fixed effect parameter, η , the drug efficacy, is surprisingly well estimated (the bias is only 0.6% and the S.E. is 2.1%).

On the other hand, if we ignore the fact that the drug is imperfect and we mistakenly fit a perfect drug model, the bias and S.E. of estimates are unacceptably large. For the same data set in this example, when we fit a perfect drug model, the bias of the population parameter estimates is as high as 17.2%, and the S.E. is as high as 39.9%. For the individual parameter estimates, the bias is as high as 78.2% and the S.E. is as high as 192.2%. Note that, when we consider the imperfect drug model, the estimates are still biased for finite sample size due to the nonlinearity, but it is asymptotically unbiased as the sample size goes to infinity.¹³ However, if the perfect drug model is used incorrectly, the bias still exists even for infinite sample size. The 95% confidence interval coverages are reasonable when we consider the imperfect drug model, but the coverages are very low when we mistakenly use the perfect drug model (Table 2).

From this example we can see that the quantification of infectious virus provides more information for the HIV dynamic parameters with protease inhibitor treatment, especially for the drug efficacy. The consequence of misapplication of the perfect drug model is serious and unacceptable when the drug efficacy parameter η is only 0.8.

To compare HNM estimation method and NLS method, we regenerated the true parameters and simulated similar data sets to those above (since the NLS method does not converge for some of the previously simulated data sets). Note that we recorded the first 100 replications for which both estimation methods converge. Both methods are used to fit the right model of infectious virus, $V_I(t)$ in (14). Table 3 summarizes the estimation results.

From the results in Table 3, we can see that the estimation bias of both methods are similar. However, the S.E. of HNM estimates are consistently smaller than those of NLS estimates for both population and individual parameters.

Table 3: The comparison results between the HNM method and NLS method with 100 replications. S.E. denotes the square root of MSE. The % is based on the true value.

Method 1: Fit $V_I(t)$ model using HNM method				
	True Value	Mean Est.	Bias (%)	S.E. (%)
Population	$c = 3.074$	3.083	0.009 (0.3%)	0.316 (10.3%)
	$\delta = 0.494$	0.493	-0.001 (-0.2%)	0.025 (5.1%)
	$\eta = 0.8$	0.801	0.001 (0.1%)	0.014 (1.8%)
Patient 1	$c = 3.81$	3.701	-0.109 (-2.9%)	0.623 (16.4%)
	$\delta = 0.26$	0.268	0.008 (3.1%)	0.031 (11.9%)
Patient 2	$c = 2.73$	2.862	0.132 (4.8%)	0.616 (22.6%)
	$\delta = 0.68$	0.678	-0.002 (-0.3%)	0.038 (5.5%)
Patient 3	$c = 3.68$	3.459	-0.221 (-6.0%)	0.471 (12.8%)
	$\delta = 0.50$	0.491	-0.009 (-1.8%)	0.034 (6.8%)
Patient 4	$c = 2.06$	2.051	-0.009 (-0.4%)	0.345 (16.7%)
	$\delta = 0.53$	0.522	-0.008 (-1.5%)	0.039 (7.3%)
Patient 5	$c = 3.09$	3.343	0.253 (8.2%)	0.469 (15.2%)
	$\delta = 0.50$	0.504	0.004 (0.8%)	0.035 (7.0%)
Method 2: Fit $V_I(t)$ model using NLS method				
Population	$c = 3.074$	3.199	0.125 (4.1%)	0.349 (11.4%)
	$\delta = 0.494$	0.494	0.000 (0.0%)	0.030 (6.0%)
	$\eta = 0.8$	0.801	0.001 (0.1%)	0.016 (2.0%)
Patient 1	$c = 3.81$	3.974	0.164 (4.3%)	0.815 (21.4%)
	$\delta = 0.26$	0.264	0.004 (1.6%)	0.035 (13.4%)
Patient 2	$c = 2.73$	2.886	0.156 (5.7%)	0.759 (27.8%)
	$\delta = 0.68$	0.687	0.007 (1.0%)	0.079 (11.6%)
Patient 3	$c = 3.68$	3.675	-0.005 (-0.1%)	0.783 (21.3%)
	$\delta = 0.50$	0.491	-0.009 (-1.8%)	0.050 (10.0%)
Patient 4	$c = 2.06$	2.178	0.118 (5.7%)	0.518 (25.2%)
	$\delta = 0.53$	0.526	-0.004 (-0.8%)	0.083 (15.6%)
Patient 5	$c = 3.09$	3.280	0.190 (6.1%)	0.767 (24.9%)
	$\delta = 0.50$	0.503	0.003 (0.6%)	0.064 (12.8%)

6. CONCLUSIONS AND DISCUSSION

In this paper, we proposed a modified model for HIV dynamics based on the results of Perelson et al.¹ These results are further exploration of Perelson et al's work¹. The hierarchical nonlinear model approach was introduced to characterize the population viral dynamics and to improve efficiency of estimation of model parameters. We showed that this approach is more powerful for identification of model misspecification since the cross-patient information is efficiently used. We also showed that the measurement of infectious virus allows us to estimate not only the viral dynamic parameters, but also the parameter that characterizes drug efficacy. From the numerical examples, the HNM procedure appears to perform well in settings where individual data are rich as well as when they are sparse. We can successfully identify the covariates for the viral dynamic parameters by the AIC or BIC criterion using the proposed approach. The simulation comparison study showed that the parameter estimates of HNM approach are superior to those from the NLS method in terms of MSE.

To apply the proposed methodology to a clinical trial, we must address several practical issues. First, we must determine what we need to measure, and how often we need to measure. Second, we must evaluate the estimation accuracy of dynamic parameters (including the clearance rates and drug efficacy) associated with a given sample size. Finally, we must determine the optimal sampling times.

Inspection of our models can help in investigating the trade-off between the use of resources to increase the number of patients and the number of measurements to take per subject. This trade-off depends on the objectives of the study. The more patients we have, the more information we obtain for estimation of the between-patient variation; the more measurements we take on each individual patient, the more information we have for estimation of the within-patient variation. If our interest is in estimating the population parameters, it may be better to have a larger number of patients with less frequent measurements per patient than to have a smaller sample size with more frequent measurements per individual. On the other hand, if our interest is in investigating the viral dynamics for individuals and the within-patient variations, we may prefer a design with a smaller sample size with frequent measurements per patient. Also notice the restrictions

for some particular studies. For example, the frequent measurements on each individual may not be practical for the study of HIV dynamics in lymphoid tissue, cerebrospinal fluid, or other compartments, or for pediatric studies. In these cases, one might recruit more patients to provide more information on population parameters. In some other studies, the number of patients may be limited due to the enrollment criteria, in which case we need frequent measurements on each individual patient to obtain sufficient information for dynamic parameter estimation.

Once we have determined the sample size and the number of measurements per individual, it is also important to determine the sampling times for each individual so as to maximize the information for parameter estimation. There are some theoretic results using D-optimal design in the literature of pharmacokinetics and other biological studies.^{19,20} These theoretic results suggested that one should replicate the measurements at a number of distinct time points which is equal to the number of parameters to be estimated. However, the optimality of this kind of design highly depends on the true model structure and the true parameter values which are unknown in most cases. The use of a sequential procedure to deal with this issue has been examined^{21,22}, but it is not convenient in practice. Most practitioners such as pharmacologists prefer intuitive (conventional) sampling schedules, that is, the sampling times are spread out in the study interval. In pharmacokinetic studies, pharmacologists usually take samples more frequently at the beginning and less frequently at the later stage. This is intuitively reasonable since the nonlinearity is more serious at the beginning of the drug dynamics and less serious at the later stage. In fact, the HIV dynamics are similar to the drug dynamics. We suggest use of a sampling schedule similar to that used in pharmacokinetic studies.

Perelson et al.¹ mentioned that the drug pharmacokinetic (drug effect) delay ranges from 2 to 6 hours. One should set the initial time of the dynamics ($t = 0$) as the starting time of drug effect and it is important to capture this starting time point. We suggest sampling as frequently as possible during the first 8 hours until one captures the drug effect time (the time that viral load starts to drop). Herz et al.⁷ provided a more complete mathematical treatment of such delay.

Since the true model structure and the true parameter values are unknown, we cannot

obtain a real optimal design. Our suggestion is to study the identifiability problem and the parameter estimation for varieties of possible models and parameter combinations using extensive Monte Carlo simulations, from which one can select a good design. Also, we notice that some measurable quantities may provide more information for parameter identification than others; we may decide what variables we should measure based on the simulation study and other considerations such as the costs.

In this paper we only considered a dynamic model for the protease inhibitor monotherapy treatment in a short time period. Our methods can be extended to include more complicated models similar to those of Perelson et al.²³ and Nowak and Bangham⁶, as well as models for multiple drug therapy. Since the current available anti-HIV agents, including protease inhibitors and reverse transcriptase inhibitors, work differently to stop virus reproduction, the effects should be modeled in different ways⁷. The assumption about constant target T cells (T) is not reasonable for a longer time-period treatment, since the CD4⁺ T cells will be recovered (at least partially) due to the treatment. This recovery implies a need for models relaxing the assumption of constant target T cell. In addition, more studies on model validation and diagnostics are needed. Although we have concentrated on the dynamic modeling of HIV infection in this paper, the methods developed in this paper may also be used to model other virus infection (such as hepatitis B virus) treated with anti-viral therapies.²⁴

APPENDIX I: PERFECT DRUG MODEL

Before treatment, we assume the system in a quasi-steady state. Setting the right sides of equations (4), (6) and (7) to be zero at initial time $t = 0$, we have

$$kTV_{I_0} = \delta T_0^* \tag{20}$$

$$(1 - \eta_0)N\delta T_0^* = cV_{I_0} \tag{21}$$

$$\eta_0 N\delta T_0^* = cV_{NI_0} \tag{22}$$

Combining (20) and (21), we get

$$kT = \frac{1}{(1 - \eta_0)} \frac{c}{N} \tag{23}$$

Substituting this and $V_0 = V_{I0} + V_{NI0}$ back into the system (20), (21) and (22), we get

$$T_0^* = \frac{c}{N\delta} V_0 \quad (24)$$

$$V_{I0} = (1 - \eta_0) V_0 \quad (25)$$

$$V_{NI0} = \eta_0 V_0 \quad (26)$$

We need to solve the following system of linear equations with the above steady-state conditions,

$$\frac{d}{dt} \begin{pmatrix} T^* \\ V_I \\ V_{NI} \end{pmatrix} = A \begin{pmatrix} T^* \\ V_I \\ V_{NI} \end{pmatrix} \quad (27)$$

with

$$A = \begin{pmatrix} -\delta & \frac{1}{(1-\eta_0)} \frac{c}{N} & 0 \\ 0 & -c & 0 \\ N\delta & 0 & -c \end{pmatrix}.$$

The eigenvalues of matrix A are $-c$ and $-\delta$, where $-c$ is a repeated eigenvalue. The corresponding eigenvector and $-c$ and $-\delta$ are

$$\begin{pmatrix} 0 \\ 0 \\ 1 \end{pmatrix}, \quad \begin{pmatrix} c - \delta \\ 0 \\ N\delta \end{pmatrix}.$$

Solving

$$\begin{pmatrix} c - \delta & \frac{c}{N} \frac{1}{1-\eta_0} & 0 \\ 0 & 0 & 0 \\ N\delta & 0 & 0 \end{pmatrix} \xi = \begin{pmatrix} 0 \\ 0 \\ 1 \end{pmatrix},$$

we have

$$\xi = \begin{pmatrix} \frac{1}{N\delta} \\ -(1 - \eta_0) \frac{c - \delta}{c\delta} \\ 0 \end{pmatrix}.$$

Therefore the solution to the system (27) is

$$\begin{pmatrix} T^* \\ V_I \\ V_{NI} \end{pmatrix} = a_1 \begin{pmatrix} c - \delta \\ 0 \\ N\delta \end{pmatrix} e^{-\delta t} + a_2 \begin{pmatrix} 0 \\ 0 \\ 1 \end{pmatrix} e^{-ct} + a_3 \left[\begin{pmatrix} \frac{1}{N\delta} \\ -(1 - \eta_0) \frac{c-\delta}{c\delta} \\ 0 \end{pmatrix} + \begin{pmatrix} 0 \\ 0 \\ 1 \end{pmatrix} t \right] e^{-ct}. \quad (28)$$

Using initial conditions (24), (25), (26), we have

$$\begin{pmatrix} \frac{c}{N\delta} \\ 1 - \eta_0 \\ \eta_0 \end{pmatrix} V_0 = \begin{pmatrix} c - \delta & 0 & \frac{1}{N\delta} \\ 0 & 0 & -(1 - \eta_0) \frac{c-\delta}{c\delta} \\ N\delta & 1 & 0 \end{pmatrix} \begin{pmatrix} a_1 \\ a_2 \\ a_3 \end{pmatrix}.$$

We derive the constants a_1 , a_2 and a_3 as

$$\begin{pmatrix} a_1 \\ a_2 \\ a_3 \end{pmatrix} = \begin{pmatrix} \frac{c^2}{N\delta(c-\delta)^2} \\ \eta_0 - \frac{c^2}{(c-\delta)^2} \\ -\frac{c\delta}{c-\delta} \end{pmatrix} V_0.$$

Substituting the above results back into (28), we have

$$\begin{pmatrix} T^* \\ V_I \\ V_{NI} \end{pmatrix} = V_0 \left[\begin{pmatrix} \frac{c^2}{N\delta(c-\delta)} \\ 0 \\ \frac{c^2}{(c-\delta)^2} \end{pmatrix} e^{-\delta t} + \begin{pmatrix} -\frac{c}{N(c-\delta)} \\ 1 - \eta_0 \\ \eta_0 - \frac{c^2}{(c-\delta)^2} \end{pmatrix} e^{-ct} - \begin{pmatrix} 0 \\ 0 \\ \frac{c\delta}{c-\delta} \end{pmatrix} t e^{-ct} \right]. \quad (29)$$

Therefore,

$$V(t) = V_0 \left\{ \frac{c^2}{(c-\delta)^2} e^{-\delta t} + \left[1 - \frac{c^2}{(c-\delta)^2} - \frac{c\delta t}{c-\delta} \right] e^{-ct} \right\},$$

which is identical to that in Perelson *et al.*¹

APPENDIX II: IMPERFECT DRUG MODEL

Using (23), the system of differential equations (4), (8) and (9) becomes

$$\frac{dT^*}{dt} = -\delta T^* + \frac{1}{(1 - \eta_0)} \frac{c}{N} V_I \quad (30)$$

$$\frac{dV_I}{dt} = (1 - \eta^*) N \delta T^* - c V_I \quad (31)$$

$$\frac{dV_{NI}}{dt} = \eta^* N \delta T^* - c V_{NI}. \quad (32)$$

Alternatively, we can write this as the form (27) with

$$A = \begin{pmatrix} -\delta & \frac{1}{(1-\eta_0)} \frac{c}{N} & 0 \\ (1-\eta^*)N\delta & -c & 0 \\ \eta^*N\delta & 0 & -c \end{pmatrix}$$

which is a constant matrix over time t .

Therefore, we can obtain the solution to this linear differential equation system by using the eigenvalue and eigenvector approach as in Appendix I. Setting $|A - \lambda I| = 0$, we obtain three eigenvalues,

$$\lambda_1 = -c, \quad \lambda_2 = \frac{-(c+\delta) + \sqrt{(c+\delta)^2 - 4c\delta\eta}}{2}, \quad \lambda_3 = \frac{-(c+\delta) - \sqrt{(c+\delta)^2 - 4c\delta\eta}}{2}.$$

Notice that for perfect drug, $\eta = 1$, we have $\lambda_1 = \lambda_3 = -c$, $\lambda_2 = -\delta$. Hence $-c$ is a repeated eigenvalue, which yields a different form of solution for the system. See Appendix I.

The corresponding eigenvectors are

$$\begin{pmatrix} 0 \\ 0 \\ 1 \end{pmatrix}, \quad \begin{pmatrix} \frac{(c-\delta) + \sqrt{(c+\delta)^2 - 4c\delta\eta}}{2N\delta} \\ (1-\eta^*) \\ \eta^* \end{pmatrix}, \quad \begin{pmatrix} \frac{(c-\delta) - \sqrt{(c+\delta)^2 - 4c\delta\eta}}{2N\delta} \\ (1-\eta^*) \\ \eta^* \end{pmatrix}.$$

Hence

$$\begin{pmatrix} T^* \\ V_I \\ V_{NI} \end{pmatrix} = a_1 \begin{pmatrix} 0 \\ 0 \\ 1 \end{pmatrix} e^{\lambda_1 t} + a_2 \begin{pmatrix} \frac{(c-\delta) + \sqrt{(c+\delta)^2 - 4c\delta\eta}}{2N\delta} \\ (1-\eta^*) \\ \eta^* \end{pmatrix} e^{\lambda_2 t} + a_3 \begin{pmatrix} \frac{(c-\delta) - \sqrt{(c+\delta)^2 - 4c\delta\eta}}{2N\delta} \\ (1-\eta^*) \\ \eta^* \end{pmatrix} e^{\lambda_3 t} \quad (33)$$

where a_1 , a_2 and a_3 are constants that we can determine from the initial conditions (24), (25), and (26),

$$\begin{pmatrix} \frac{c}{N\delta} \\ 1 - \eta_0 \\ \eta_0 \end{pmatrix} V_0 = \begin{pmatrix} \frac{(c-\delta)(a_2+a_3) + \sqrt{(c+\delta)^2 - 4c\delta\eta}(a_2-a_3)}{2N\delta} \\ (1-\eta^*)(a_2+a_3) \\ a_1 + \eta^*(a_2+a_3) \end{pmatrix}.$$

Hence

$$\begin{cases} a_1 = -\frac{\eta}{1-\eta}V_0, \\ a_2 = \frac{V_0}{2(1-\eta)}\left[1 + \frac{\delta+c-2c\eta}{\sqrt{(c+\delta)^2-4c\delta\eta}}\right], \\ a_3 = \frac{V_0}{2(1-\eta)}\left[1 - \frac{\delta+c-2c\eta}{\sqrt{(c+\delta)^2-4c\delta\eta}}\right]. \end{cases} \quad (34)$$

Then the final solution is

$$\begin{aligned} T^* &= \frac{T_0^*}{2} \left[\left(1 + \frac{c+\delta}{\sqrt{(c+\delta)^2-4c\delta\eta}}\right) \exp\left(\frac{-(c+\delta)+\sqrt{(c+\delta)^2-4c\delta\eta}}{2}t\right) \right. \\ &\quad \left. + \left(1 - \frac{c+\delta}{\sqrt{(c+\delta)^2-4c\delta\eta}}\right) \exp\left(\frac{-(c+\delta)-\sqrt{(c+\delta)^2-4c\delta\eta}}{2}t\right) \right] \\ V_I &= (1-\eta^*)\frac{V_0}{2(1-\eta)} \left[\left(1 + \frac{\delta+c-2c\eta}{\sqrt{(c+\delta)^2-4c\delta\eta}}\right) \exp\left(\frac{-(c+\delta)+\sqrt{(c+\delta)^2-4c\delta\eta}}{2}t\right) \right. \\ &\quad \left. + \left(1 - \frac{\delta+c-2c\eta}{\sqrt{(c+\delta)^2-4c\delta\eta}}\right) \exp\left(\frac{-(c+\delta)-\sqrt{(c+\delta)^2-4c\delta\eta}}{2}t\right) \right], \\ V_{NI} &= \eta^*\frac{V_0}{2(1-\eta)} \left[\left(1 + \frac{\delta+c-2c\eta}{\sqrt{(c+\delta)^2-4c\delta\eta}}\right) \exp\left(\frac{-(c+\delta)+\sqrt{(c+\delta)^2-4c\delta\eta}}{2}t\right) \right. \\ &\quad \left. + \left(1 - \frac{\delta+c-2c\eta}{\sqrt{(c+\delta)^2-4c\delta\eta}}\right) \exp\left(\frac{-(c+\delta)-\sqrt{(c+\delta)^2-4c\delta\eta}}{2}t\right) \right] - \frac{\eta V_0}{(1-\eta)} \exp(-ct). \end{aligned} \quad (35)$$

Notice that $\eta = (\eta^* - \eta_0)/(1 - \eta_0)$, thus $\eta^* = \eta(1 - \eta_0) + \eta_0$ and $(1 - \eta^*)/(1 - \eta) = 1 - \eta_0$, and also using (25) and (26), we obtain,

$$\begin{aligned} V_I(t) &= \frac{V_{I0}}{2} \left[\left(1 + \frac{\delta+c-2c\eta}{\sqrt{(c+\delta)^2-4c\delta\eta}}\right) \exp\left(\frac{-(c+\delta)+\sqrt{(c+\delta)^2-4c\delta\eta}}{2}t\right) \right. \\ &\quad \left. + \left(1 - \frac{\delta+c-2c\eta}{\sqrt{(c+\delta)^2-4c\delta\eta}}\right) \exp\left(\frac{-(c+\delta)-\sqrt{(c+\delta)^2-4c\delta\eta}}{2}t\right) \right], \\ V_{NI}(t) &= \frac{\eta V_{I0} + V_{NI0}}{2(1-\eta)} \left[\left(1 + \frac{\delta+c-2c\eta}{\sqrt{(c+\delta)^2-4c\delta\eta}}\right) \exp\left(\frac{-(c+\delta)+\sqrt{(c+\delta)^2-4c\delta\eta}}{2}t\right) \right. \\ &\quad \left. + \left(1 - \frac{\delta+c-2c\eta}{\sqrt{(c+\delta)^2-4c\delta\eta}}\right) \exp\left(\frac{-(c+\delta)-\sqrt{(c+\delta)^2-4c\delta\eta}}{2}t\right) \right] - \frac{\eta V_0}{(1-\eta)} \exp(-ct). \end{aligned} \quad (36)$$

ACKNOWLEDGMENT

This work was partially supported by the Statistical and Data Analysis Center of the AIDS Clinical Trials Group, under the National Institute of Allergy and Infectious Diseases contract No. U01 AI38855. We thank Scott Hammer, Daniel Kuritzkes and Michael Lederman for discussions on virology issues. We also thank the editor and two referees for their suggestions and comments.

REFERENCES

1. Perelson, A.S., Neumann, A.U., Markowitz, M., Leonard, J.M. and Do, D.D. 'HIV-1 dynamics in vivo: virion clearance rate, infected cell life-span, and viral generation time', *Science*, Vol. 271, 1582-1586 (1996).
2. Ho, D.D., Neumann, A.U., Perelson, A.S., Chen, W., Leonard, J.M. and Markowitz, M. 'Rapid turnover of plasma virions and CD4 lymphocytes in HIV-1 infection', *Nature*, Vol. 373, 123-126 (1995).
3. Wei, X., Ghosh, S.K., Taylor, M.E., Johnson, V.A., Emini, E.A., Deutsch, P., Lifson, J.D., Bonhoeffer, S., Nowak, M.A., Hahn, B.H., Saag, M.S. and Shaw, G.M. 'Viral dynamics in human immunodeficiency virus type 1 infection', *Nature*, Vol. 373, 117-122 (1995).
4. De Jong, M.D., Veenstra, J., Stilianakis, N.I., Schuurman, R., Lange, J.M.A., De Boer, R.J. and Boucher, C.A.B. 'Host-parasite dynamics and outgrowth of virus containing a single K70R amino acid change in reverse transcriptase are responsible for the loss of human immunodeficiency virus type 1 RNA load suppression by zidovudine', *Proc. Natl. Acad. Sci. USA*, Vol. 93, 5501-5506 (1996).
5. De Boer, R.J. and Boucher, C.A.B. 'Anti-CD4 therapy for AIDS suggested by mathematical models', *Proceedings of the Royal Society of London- Series B: Biological Sciences*, 263 (1372), 899-905 (1996).
6. Nowak, M.A. and Bangham, C.R.M. 'Population dynamics of immune responses to persistent viruses', *Science*, Vol. 272, 74-79 (1996).
7. Herz, A.V.M., Bonhoeffer, S., Anderson, R.M., May, R.M., and Nowak, M.A. 'Viral Dynamics in Vivo: Limitations on Estimates of Intracellular Delay and Virus Decay', *Proc. Natl. Acad. Sci. USA*, 93, 7247-7251 (1996).
8. Nowak, M.A., Bonhoeffer, S., Shaw, G. and May, R.R. 'Anti-viral drug treatment: dynamics of resistance in free virus and infected cell populations', *Journal of Theoretical Biology*, 184, 203-217 (1997).

9. Bonhoeffer, S., May, R.M., Shaw, G.M. and Nowak, M.A. 'Virus dynamics and drug therapy', *Proc. Natl. Acad. Sci. USA*, 94, 6971-6976 (1997).
10. Piatak, M., Saag, M.S., Yang, L.C., Clark, S.J., Kappes, J.C., Luk, K.-C., Hahn, B.H., Shaw, G.M., and Lifson, J.D. 'High levels of HIV-1 in plasma during all stages of infection determined by competitive PCR', *Science*, 259, 1749-54 (1993).
11. McKeating, J.A. and Moore, J.P. 'HIV infectivity', *Nature*, 349: 660 (1991).
12. Bourinbaiar, A.S. 'HIV and gag', *Nature*, 349: 111 (1991).
13. Davidian, M. and Giltinan, D.M. Nonlinear models for repeated measurement data, Chapman & Hall, New York, 1995.
14. Steimer, J.L., Mallet, A., Golmard, J.L. and Boisvieux, J.F. 'Alternative approaches to estimation of population pharmacokinetic parameters: comparison with the non-linear mixed-effect model', *Drug Metabolism Reviews*, 15 (1&2), 265-292 (1984).
15. Sheiner, L.B., Rosenberg, B. and Marathe, V.V. 'Modeling of individual pharmacokinetics for computer-aided drug dosing', *Computers and Biomedical Research*, 5, 441-459 (1972).
16. Rowland, M., Sheiner, L.B. and Steimer, J.L. Variability in drug therapy, description, estimation, and control, Raven Press, New York, 1985.
17. Steimer, J.L., Mallet, A. and Mentre, F. 'Estimating Interindividual pharmacokinetic variability', In *Variability in drug therapy, description, estimation, and control*, ed. Rowland et al., 65-109 (1985).
18. Pinheiro, J.C. and Bates, D.M. Mixed-Effects Models Methods and Classes for S and Splus, downloaded from "<ftp://ftp.stat.wisc.edu/src/NLME/Unix>", 1995.
19. Landaw, E.M. 'Optimal design for individual parameter estimation in pharmacokinetics', In *Variability in drug therapy, description, estimation, and control*, ed. Rowland et al., 187-198 (1985).

20. Landaw, E.M. and DiStefano, J.J. 'Multiexponential, multicompartmental, and non-compartmental modeling. II. Data analysis and statistical considerations', *Am. J. Physiol.*, 246, R665-R677 (1984).
21. DiStefano, J.J. 'Optimized blood sampling protocols and sequential design of kinetic experiments', *Am. J. Physiol.*, 240, R259-R265 (1981).
22. D'Argenio, D.Z. 'Optimal sampling times for pharmacokinetic experiments', *Journal of Pharmacokinetics and Biopharmaceutics*, Vol. 9, No. 6, 739-756 (1981).
23. Perelson, A.S., Kirschner, D.E. and Boer R.D. 'Dynamics of HIV infection of CD4⁺ T cells', *Mathematical Biosciences*, 114, 81-125 (1993).
24. Nowak, M.A., Bonhoeffer, S., Hill, A.M., Boehme, R., Thomas, H.C. and McDade, H. 'Viral dynamics of HBV infection', *Proc. Natl. Acad. Sci. USA*, 93, 4398-4402 (1996).